Reversible shape changes of the end facet on Schottky electron emitters

M. S. Bronsgeest and P. Kruit[a)]
Delft University of Technology, Lorentzweg 1, 2628 CJ Delft, The Netherlands

(Received 9 July 2009; accepted 24 August 2009; published 1 December 2009)

The Schottky electron source is predominant in today's focused electron-beam equipment, but its properties are still not fully understood. Generally, its performance is predicted, assuming its tip end geometry is known and stable. In this work, it is shown that the size of the end facet (slowly) shrinks upon reduction in the extraction voltage and (more rapidly) grows upon restoration of the original voltage. Furthermore, the shape of the end facet could be made to change from more circular to octagonal or more squarish. These changes affect the properties of the beamlet that will be cut from the facet beam for practical applications. Better knowledge of the *in situ* shape of the emitter allows for a better prediction of its performance and stability. © *2009 American Vacuum Society.*
[DOI: 10.1116/1.3237145]

I. INTRODUCTION

The Schottky electron source[1] is predominant in today's focusing electron beam equipment, such as electron microscopes and lithography machines. It is operated at high temperature (1800 K) and in an electric field close to 1 V/nm. The source (Fig. 1) consists of an etched single crystalline tungsten wire of 1 mm long, 125 μm in diameter, with {100} planes perpendicular to the wire axis. The tip end is of the order of a micron in diameter and has a {100} facet at the tip end of several hundred nanometers in diameter.

The beam or probe current used in an electron microscope or lithography machine is the central part of the beam that is emitted by this facet. To reduce the work function of the bare W{100}, a reservoir of ZrO_x is attached to the wire halfway along its length. At the operating temperature, the zirconium and oxygen diffuse along the wire to reach the tip end and enhance the electron emission.

For applications such as lithography machines and (scanning) (transmission) electron microscopes [(S)(T)EM] the relevant parameters are the brightness, energy spread, and the angular current density of the central beamlet from the facet. The angular intensity is a practical issue: how much current is cut by a beam-limiting aperture, while the former two are of a more fundamental nature and determine the minimum size of the probe that can be formed with the selected beam current [S(T)EM], or the coherence of the beam (TEM).

Both brightness and energy spread depend on the field strength at the emitting end facet. The local field strength is a function of the applied voltages, the gun configuration, and the shape and size of the tip. These same parameters also determine the lens effect between the tip and the extractor, which affects the translation of the current density on the emitter surface into the angular intensity of the beam through the system.

To provide a stable beam with constant properties, any changes in the tip geometry should be prevented. It is known, however, that the shape of a Schottky electron source in operation can change in time. Shape changes become particularly important when probe properties need to be constant over a long time period (lithography applications), and/or when a larger area of the end facet is of interest, such as for multibeam applications.[2]

In a previous paper[3] we have focused on the typical collapsing of the tip end. In this article, we would like to report on typical changes of the tip end without the collapsing of the facet itself.

The emission patterns from Schottky (Zr/O/W) emitters available in literature are circular,[1] and it is usually assumed the facet is also circular. In fact, simulations for rotationally symmetric emitters, with spherical tip ends truncated by a facet with a diameter of $0.6r_{\text{tip}}$, have yielded the equations that are now commonly used to calculate the beam properties based on the gun geometry and the applied potentials.[1] In practice, the facet size can be different from $0.6r_{\text{tip}}$, and also its geometry is not necessarily circular, as shown in Fig. 2. We have investigated the response of the end facet of a commercial Schottky electron source in terms of facet size and shape by recording the evolution of the emission pattern and currents for different operating conditions and will discuss the practical consequences.

Section II addresses the question why the facet would change upon a change in the operation conditions. Section III gives the experimental details, and the interpretation of the emission pattern is discussed in Sec. IV. In Sec. V we present results, which are discussed in Sec. VI. Conclusions follow in Sec. VII.

II. WHY WOULD AN EMITTER TIP CHANGE ITS SHAPE?

In the following it will be assumed that an emitter tip can be considered to be a "crystallite," supported by the emitter cone. This allows us to borrow results from the equilibrium crystal shape theory for "free" crystallites.

A free crystallite will try to adopt its equilibrium crystal shape if it is heated to a temperature that allows for diffusion to occur. The equilibrium shape is the shape that gives the lowest total surface free energy for the thermodynamic sys-

[a)]Electronic mail: p.kruit@tudelft.nl

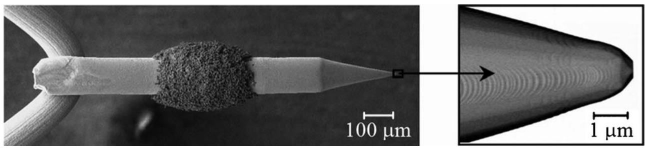

FIG. 1. SEM images of a Schottky emitter. Left: with the ZrO_x reservoir and the legs for resistive heating. Right: close-up of tip end.

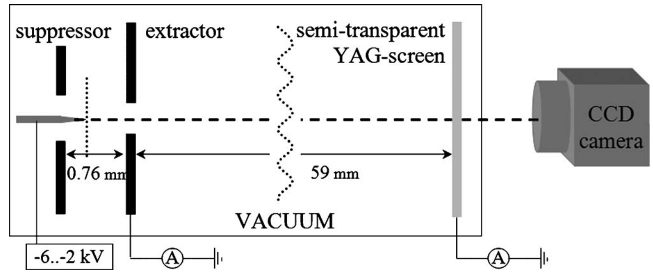

FIG. 3. Schematic drawing of the experimental setup.

tem considered. The total surface free energy is a function of the natural variables of the system, such as temperature and applied potential. The equilibrium shape of a crystallite can be found from a so-called Wulff plot if the dependence of the specific surface free energy (surface free energy per area) on the crystallographic orientation is known. The variations in specific surface free energy change with the applied conditions: upon heating a crystallite the anisotropy in specific surface energy will diminish, and the equilibrium shape will become more spherical,[4] and upon applying a potential the anisotropy in specific surface energy will increase, and the equilibrium shape will become more faceted.[5]

Already in 1965 Nichols and Mullins[6] reported of a discussion in literature as to what extent a tip will adopt the equilibrium crystal shape of a free crystallite of equivalent size. This is because for a "supported" crystallite such as an emitter tip, the net atom transport is possible between the crystallite and the "support structure:" the emitter cone. The emitter as a whole generally has a nonequilibrium shape. The shape evolution of heated emitters was described by assuming local equilibrium between bulk and surface.[6,7] This allows for the definition of a local surface chemical potential. In equilibrium, the chemical potential gradient is zero everywhere, but variations in the surface chemical potential yield net mass transport that changes the shape. For a typical emitter geometry, the atoms at the sharp tip have a higher chemical potential than those along the shank so that at elevated temperatures the tip atoms will tend to migrate along the emitter axis from the apex toward the shank to reduce the emitter length and decrease the tip curvature. Experimentally it was found that the mechanism involved was repetitive collapse of the end facet. In this process atoms detach from the perimeter of the facet, making the top layer(s) smaller in diameter and exposing the larger diameter layer underneath. The detached atoms reattach elsewhere. This mechanism is also seen for free crystallites that evolve from a more spherical shape toward a more faceted shape.

For a Schottky emitter in operation, there is an electric field at the emitter surface, which is strong at the tip end and decreases to zero somewhere on the conical part (depending on the suppressor voltage). This decreases the chemical potential at the tip end with respect to that for the shank area.[7] For strong field gradients, the direction of the chemical potential gradient can even be reversed: in that case atoms are transported from the shanks toward the tip.

Barbour *et al.*[7] derived an equation for the field strength that would give zero gradient in the tip area and thus (local) geometrical stability. This field depends on the tip size and the (averaged) surface tension of the material. Zero gradient in the tip area, however, does not ensure full stability of the emitter as a whole because the gradient is not necessarily zero everywhere on the emitter.[8]

The behavior of the tip end is thus a function of the local variations in chemical potential on the tip end itself and the difference in chemical potential between the tip end and the remaining part of the emitter. This interplay was seen experimentally, e.g., by Barbour *et al.*,[7] Bettler and Love,[9] and more recently by Fujita and Shimoyama,[5] who all have investigated single crystalline tungsten needles with a tip radius of $10^{-1}-10^{0}$ μm. Contrary to the other works, Fujita and Shimoyama[5] investigated changes in the tip shape for which the end facet did not collapse. They showed the degree of faceting on the tip end changed with the applied voltage, but they also noted that the size of the tip end gradually grew during their experiments. This confirms that the geometry of the tip end is a delicate interplay between effects on two different length scales. In this article, we investigate how this works out for a Schottky emitter, the predominant electron source in today's electron-beam equipment: also a single crystalline tungsten emitter, but with zirconium and oxygen present on the surface. As Fujita and Shimoyama[5] we will prevent "collapsing rings,"[1,3] but in contrast to their work the bias will be reversed: the field is applied by biasing the emitter negatively with respect to an "extractor" electrode. This allows us to monitor changes *in situ* by looking at the emission pattern.

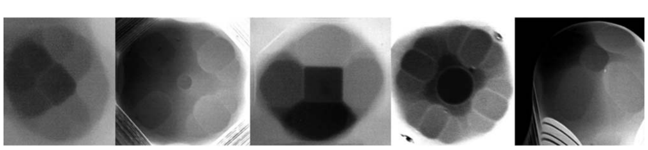

FIG. 2. Top down SEM images of Schottky emitters with different facet geometries, generated by operating at different conditions.

III. EXPERIMENT

The experiments have been performed with a commercial Zr/O/W(100) Schottky source (Fig. 1) supplied with suppressor cap and heating wire.[10] The source was operated in the setup given schematically in Fig. 3. The emitter was mounted on a vacuum system with a background pressure of $\sim 1\times 10^{-7}$ Pa. In operation the pressure increased but was always below 1×10^{-6} Pa. The emitter was heated by run-

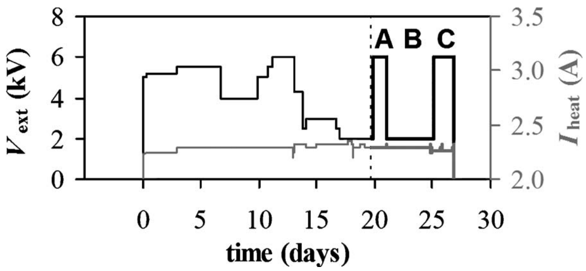

FIG. 4. Operation conditions applied to the emitter during the experiments. Vertical dashed line marks the start of the experiments discussed in this article.

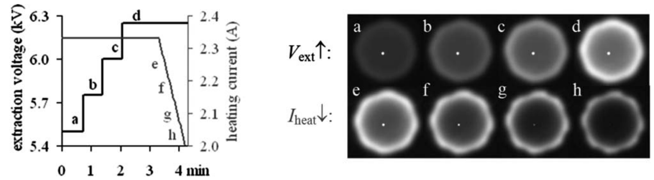

FIG. 5. Effect of the operating conditions on the emission pattern. N.B. Central bright spot in the patterns is light emitted by the hot source, penetrating the YAG screen. All patterns are recorded with the same camera settings.

ning a current through the heating wire (Fig. 1). The relation between current and source temperature has been calibrated by the manufacturer. For most of the time we have operated the emitter predominantly at 2.27–2.33 A, which corresponds to a temperature range of 1740–1810 K in the test system of the manufacturer. Because we have mounted the emitter in a different setup, the true temperature range might be slightly different.

At room temperature the emitter cone protrudes 249 μm from the suppressor cap (hole diameter of 600 μm). The emitter protrusion will increase upon heating due to thermal expansion, with 30–40 μm. Opposite to the suppressor at 0.76 mm was a grounded extractor plate with a hole of 400 μm in diameter. This configuration will transit all of the beam emitted by the end facet, but will block emission from other {100} areas that are present on the emitter surface. By applying a voltage to the suppressor that is negative with respect to the emitter, emission from parts other than the cone is suppressed. The suppressor voltage was kept at −0.3 kV with respect to the emitter at all times. The extraction voltage was applied by bringing down the potential of the emitter with respect to the extractor. The potential difference has been varied between 2 and 6 kV.

The effect of the operation conditions on the facet size and shape was investigated by monitoring the emission pattern generated by the end facet. To image the emission pattern, there was a grounded semitransparent yttrium aluminum garnet (YAG) screen at 59 mm behind the extractor plate. The energy of the beam that hits the YAG screen is determined by the extraction voltage. Outside the vacuum the emission pattern was recorded through a view port with a charge-coupled device (CCD) camera.

To support the interpretation of emission patterns, SEM images have been used. Also, in addition to the emission pattern, the current in the pattern was measured, collected on the YAG screen, as was the current collected on the extractor plate, and the total emission leaving the source.

To induce changes of the end facet, we have applied different operating conditions during slightly less than a month of operation. Figure 4 shows the applied conditions as a function of time. For clarity, the short term variations have been omitted in this figure. In the third week the operating voltage was kept low. The situation at the end of the third week is the starting point for the results discussed in this article. In the final week the extraction voltage was increased for about a day (section A), reduced again for several days (section B), and finally increased again for almost 2 days (section C). It was verified that all reported changes were achieved without a single collapse of the end facet.

IV. INTERPRETATION OF THE EMISSION PATTERN

The emission pattern can be seen as a blurred and distorted "shadow image" of the emitting surface. A shadow because the emission appears to be coming from a point inside the emitter behind the emitting surface: the virtual source. Blurred because the hot surface emits electrons with a distribution of tangential energies. Distorted because the lens between the emitting surface and the extractor has aberrations. The "thermal" blur is of the order of ~30 nm. This is because the distribution of tangential energies of the emitted electrons gives the beam a finite virtual source with a FW50 (full width containing 50% of the current) of ~30 nm at ~30 μm behind the facet. The distortion can be a much stronger effect. The lens aberrations can considerably change the spatial current density distribution between the facet plane and the plane of the screen where we record it.

The best "image" of the facet geometry is obtained at a relatively high extraction voltage and a relatively low temperature. At low extraction voltage the absolute field variation across the facet is small and with that also the current density variation across the facet. In that case the effect of the facet-extractor lens aberration dominates the pattern and as a result all "facet features" in the pattern are lost: at very low voltage the pattern approximates a Gaussian.[1] Figure 5 gives an experimental series to show the effect of the extraction voltage on the pattern, recorded at constant camera settings. The example does not extend down to the voltage that gives more Gaussian distributions because the voltage range for which the pattern can be detected without changing the camera settings is limited. The same figure also includes the effect of a change in heating current. As can be seen the absolute current density variations across the facet become larger at lower temperatures. This can be explained with a temperature dependence of the work function.[11]

With respect to the interpretation of pattern size, it is further noted that the size of the pattern is not only affected by the size of the facet but also by the geometry of the emitter behind the facet. This is because the geometry of the emitter behind the facet affects the field strength and field strength variation across the facet and also the facet-extractor lens

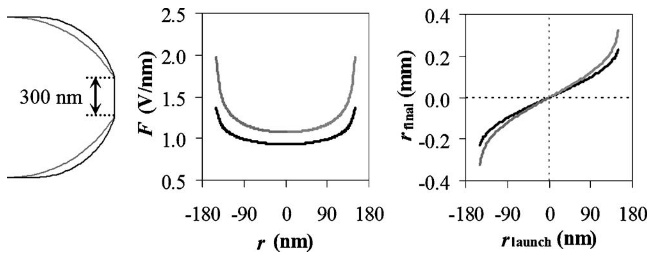

FIG. 6. Tip geometry behind the facet affects the field across the facet and the facet-extractor lens properties. Left: two different geometries with equivalent facet diameters, center: the field across the facet for the given geometries, and right: the relation between the distance from the optical axis of the launch position on the facet, and the position at a plane in the field free zone behind the extractor (at 2.5 mm from the facet). For the calculation, the gun geometry in Fig. 3 was used with 0.26 mm protrusion, a suppressor voltage of −0.3 kV and an extraction voltage of 5.5 kV. Ray tracing and field evaluation details in Ref. 12.

strength and its spherical aberration. An example is given in Fig. 6. A change in the pattern size is thus not automatically an equivalent change in the facet size, but can also be induced by, e.g., sharpening of the facet edge.

V. RESULTS

The emission pattern at the end of the third week, in which the operating voltage was kept low, is the first pattern given in Fig. 7. The pattern is taken at an extraction voltage of 6 kV and a heating current of 2.29 A. Starting from this pattern, the operating voltage was kept at 6 kV for 27 h. Figure 7 gives the evolution of the emission pattern. It can be seen that upon increasing the extraction voltage to 6 kV after prolonged operation at low extraction voltage, the emission pattern starts to increase in size and changes in shape. Figure 8 gives the current in the pattern as a function of time. Upon increasing the extraction voltage, the facet current increases from 26 to 43 μA (165%) in 15 h. Also, after 17 h the pattern and current in the pattern appear to be stabilized. Figure 8 also shows that while the total facet current increases, the intensity at the center of the pattern, relevant for (single beam) applications, decreases. The third graph in Fig. 8 gives the extractor current profile. The current collected on the extractor at $t=0$ is 71 μA and 62 μA at 20 h. The changes are significant, but its trend is currently not understood.

The extraction voltage was now reduced for several days (section B in Fig. 4). Figure 9 shows two emission patterns recorded at 6 kV and 2.29 A: the first is taken just before reducing the extraction voltage, and the second after 88 h of operation at 2 kV. It can be seen that the pattern returns to a shape and size similar to the first pattern in Fig. 7. The current in the second pattern in Fig. 9 is 27 μA, compared to 26 μA in the similar looking Fig. 7(a) pattern. Figure 10 gives the current collected on the screen and the variation in the extractor current during the operation at 2 kV. The screen current in Fig. 10 shows no sign of stabilization at 88 h and it is expected that for prolonged operation at 2 kV the facet will eventually collapse. Furthermore, it is noted that the variation in the extractor current shows a trend opposite to that seen in Fig. 8.

Finally, the extraction voltage is increased again to 6 kV (section C in Fig. 4). Figure 11 shows the emission patterns at 0, 5, 10, and 15 h after setting the voltage back to 6 kV. The screen current and the variation in the intensity at the pattern center and in the extractor current have been given in Fig. 8, in gray. The screen current increases from 27 to 38 μA (up by 141%). As before, the screen current seems to be stabilized, but this time after 15 h. This was now further investigated. The emitter was operated at 6 kV for 43 h in

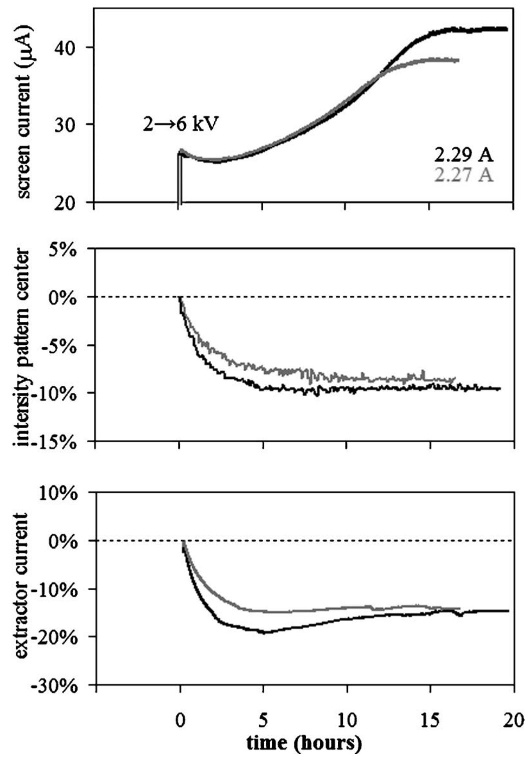

FIG. 8. Response upon increasing the extraction voltage from 2 to 6 kV after prolonged operation at low voltage. Black curves correspond to section A in Fig. 4 (patterns in Fig. 7) and gray curves correspond to section C in Fig. 4 (patterns in Fig. 11). Top: the current collected on the YAG screen. Center: the relative change in the intensity of the pattern center. Bottom: the variation in current collected on the extractor.

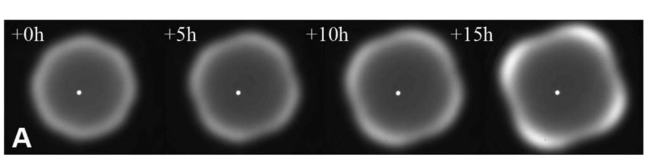

FIG. 7. Emission patterns at 6 kV, 2.29 A, taken at 0, 5, 10, and 15 h after setting the extraction voltage to 6 kV.

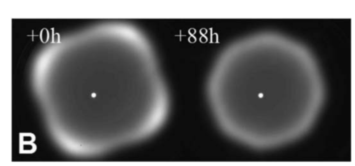

FIG. 9. Emission patterns at 6 kV, 2.29 A (top), and low temperature (bottom). Right ones are after operating at 2 kV for 88 h.

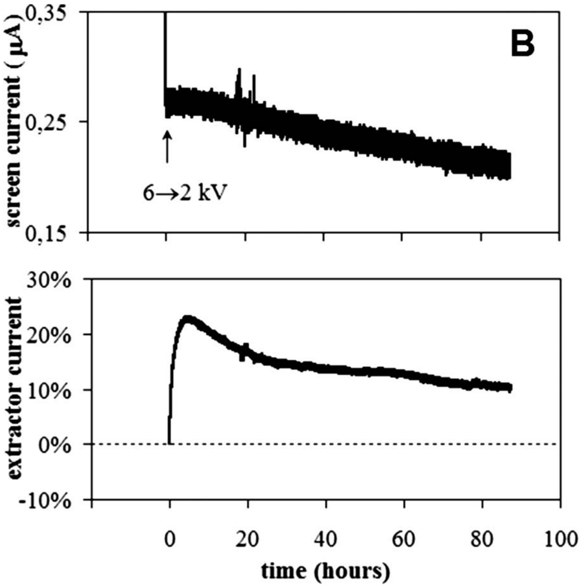

FIG. 10. Response upon decreasing the extraction voltage from 6 to 2 kV. Top: the current collected on the YAG screen. Center: the relative change in the current collected on the extractor.

total, with occasional short term variations. It was found that the facet current and the intensity in the pattern center for constant conditions remained constant within 1%.

As a check of the reproducibility the emitter was temporarily heated to 2.29 A and the pattern was compared to the stabilized pattern in Fig. 7. It was found that the size and geometry of the contour (same intensity contour line) were equivalent, but that the current in the pattern taken first was a few percent higher.

To get a slightly sharper image of the facets the temperature has occasionally been reduced during the experiments. Figure 12 gives such cold patterns at the beginning and end of sections A, B, and C. Figure 12 shows that both patterns that develop for low voltage operation (patterns 1 and 3) and for high voltage operation (patterns 2 and 4) are reproducible.

VI. DISCUSSION

Geometric changes

For the interpretation of the changes in the emission patterns in terms of the tip end geometry, we first go back to the start of the experiments. Figure 13 gives the SEM image of the initial as-purchased tip end geometry and the emission

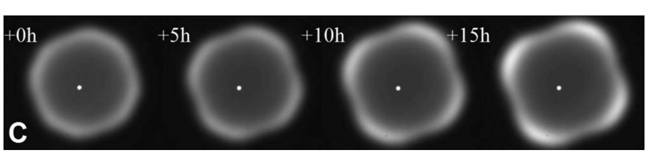

FIG. 11. Emission patterns at 6 kV, 2.27 A. 0, 5, 10, and 15 h after changing the voltage from 2 to 6 kV.

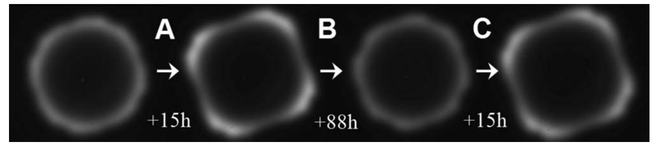

FIG. 12. Emission patterns taken by temporarily reducing the heating current to ~1.97 A at a voltage of 6 kV, after prolonged operation at low (patterns 1 and 3) or high extraction voltage (patterns 2 and 4) at normal operating temperatures.

pattern that was recorded right after starting up the source. The tip end geometry in Fig. 13 is the result of a stabilization routine performed by the manufacturer.

The emission pattern in Fig. 13 shows an octagonal facet shape, with a dark ring. The dark ring indicates the presence of a circular {100} island on the facet.[1,3] We do not expect this island to be formed during the start up of the source because the source temperature has not been high enough yet. We thus assume that the island must have been present upon purchase and has only a small height because it is not visible on the side view SEM image in Fig. 13. It collapsed to disappear in the first 10 days of operation of the source. The octagonal shape of the emission pattern can be associated with the faceted tip end geometry seen in the SEM image in Fig. 13. The facets meeting the front facet correspond to low index faces of the crystal; the {110} and {211} planes, which make angles with the {100} front facet of, respectively, 45° and 35°. The side view SEM image suggests the edges of the {100} front facet touching the {110} facets are shorter than the edges touching the {211} facets, which would mean that for the emission pattern in Fig. 13 the edges with the {110} facets are as indicated.

For prolonged operation at lower field the tip shape is expected to become more spherical, with both rough regions and (small) low-index facets, while for prolonged operation at higher field the tip shape is expected to become more faceted, with larger (and possibly fewer) facets and sharper edges and corners. To quantify "lower" and "higher" field for the as-purchased emitter geometry, we need to know the field for which it was stabilized. The stabilization routine by the manufacturer was done in a similar gun geometry as shown in Fig. 3, at a final extraction voltage of 6.745 kV, a suppressor voltage of −240 V, and at a heating current of 2.32 A (1800 K). Translating the applied potentials to a field

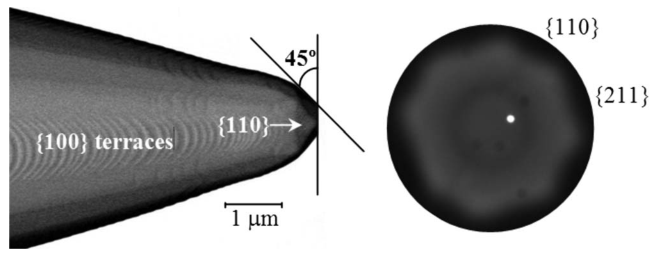

FIG. 13. SEM image of the tip of the Schottky electron emitter before the experiments[10] and the emission pattern after starting up the source. Dark spots in pattern are stains on CCD camera lens. Pattern recorded at 5 kV extraction voltage, and a heating current of 2.20 A.

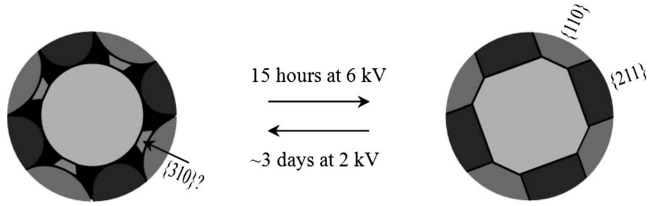

FIG. 14. Top down view of suggested tip end geometry for prolonged operation at 2 kV (left) and 6 kV (right).

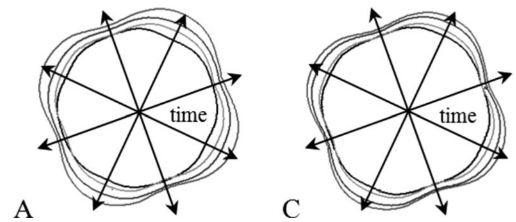

FIG. 15. Overlays of the contours of constant intensity for the emission patterns in Fig. 7 (section A) and 11 (section C).

strength at the emitter surface is not that straightforward, but if the tip and gun geometry are known, a suitable method is a "charge density" or "boundary element" method.[12] We approximate the emitter in Fig. 13 with a rotationally symmetric geometry that is based on the contour of the SEM image and use the gun geometry as in Fig. 3. The tip protrusion is set at 0.28 mm to take into account thermal expansion. This gives a field strength at the facet center, associated with the stabilization conditions, of ~1.15 V/nm. In the experiment the suppressor voltage was −300 V and the extraction voltage was 2–6 kV. The associated field range is calculated to be ~0.3–1.1 V/nm. The lowest field applied in the experiment is thus lower than the stabilization conditions, while the highest field is close to the field associated with the stabilized geometry in Fig. 13. Note that the calculated fields should be considered approximates: the true tip shape is not rotationally symmetric, the thermal expansion is not known exactly, and it is expected that the emitter geometry as a whole evolves over time.

Based on patterns 2 and 4 in Fig. 12, and taking into account that the applied field strength is close the field strength associated with Fig. 3, it is believed that for prolonged operation at 6 kV the tip end is fully faceted, consisting of {211} and {110} planes connected to the octagonal {100} end facet, as it was upon purchase. A top down view of the suggested tip end geometry is given in Fig. 14 (right), in close agreement with the first SEM image of Fig. 2. A fully faceted geometry could explain the fact that the pattern is stabilized (at least temporarily): to further increase the end facet size would require (some of) the connecting end facets to expand outward, which is a process that generally involves a nucleation barrier. An example of this is believed to be the threshold voltage found by Fujita and Shimoyama[5] that marked a sudden transition from a fully faceted tungsten tip end with {110} and {211} facets connecting to the {100} end facet to one with only {110} facets connecting to the {100} facet. A similar transition is expected for the Schottky emitter for operation at extraction voltages above 6 kV. (Also for operation at very high fields it is speculated that microprotrusions might form.[5,13])

Note that by changing the operating voltage from low to high, the net diffusion from tip to shank is reduced, stopped, or even reversed, depending on the variation in curvature and field strength along the surface. This will lead to a change in the geometry behind the tip end, which eventually could destabilize the tip end. Clear evidence of tip growth during the experiments was not observed, but an indication of tip growth, and thus a reduction in the average field enhancement factor, is the fact that the total facet current at a heating current of 2.29 A, after prolonged operation at 6 kV, is roughly 10% lower the second time (C, compared to A).

For prolonged operation at low extraction voltage, the pattern is smaller than the patterns after operation at 6 kV. The pattern shape is approximately circular, although there also might be facets connecting to the end facet, which could explain the four straight sections in between peaks of slightly increased intensity along the perimeter of the pattern. The smaller and more circular pattern geometry is in agreement with a more spherical tip end with smaller facets connected by rough regions, as expected for operation at low fields. The straight sections on the perimeter might be associated with the presence of {310} planes, which make a much smaller angle with the end facet than the {110} planes, but this cannot be confirmed. Note that the intensity along the perimeter of the pattern is more uniform in patterns 1 and 3 than in patterns 2 and 4. The top down view of a possible geometry has been given in Fig. 14. For operation at low voltage, the end facet is expected to collapse at some point, in response to the gradient in chemical potential which promotes net diffusion away from the sharp tip. The fact that there was no sign of stabilization is in agreement with this.

To get a better impression of how the tip end evolves, Fig. 15 gives overlays of contour lines of equivalent intensity, from the four images in Figs. 7 (section A) and 11 (section C). It can be seen that the pattern expands very little toward the {211} planes and much more toward the {110} planes. The expansion toward the {211} planes might be the result not of a radial expansion of the end facet in that direction but of sharpening of the facet edge: the rough sections are filled up, the {211} planes expand, and the ridges that separate the {211} planes from the end facet increase in length. This would make the pattern slightly larger (see, e.g., Fig. 6). The expansion of the pattern toward the {110} planes is larger, and this is considered to be more likely the result of also some radial expansion of the facet, in addition to the effect of edge sharpening.

Changing from the low voltage to the high voltage pattern occurred much faster than changing from the high voltage to the low voltage pattern. This is not fully understood. Possibly this is related to the difference in the amount of rough area present on the tip end between the low voltage and the high voltage shape affecting diffusion rates, and/or the dif-

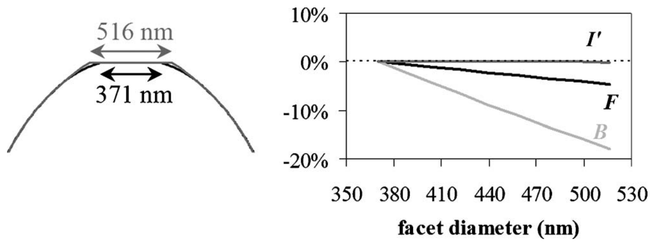

FIG. 16. Calculated change in field strength F at the facet center, brightness B, and angular current density I', for a facet growth as indicated on the left, for operation at a constant voltage. Field strength for 371 nm facet is 1.0 V/nm. Calculated for the gun geometry of Fig. 3 with 0.28 mm protrusion, a suppressor voltage of -0.3 kV and an extraction voltage of 6 kV. Ray tracing, field evaluation details in Ref. 12.

ference in the strength of the chemical potential gradient in the tip vicinity, between low and high voltage operations.

Practical consequences

The changes in facet size affect two parameters relevant to the performance of microscopes and lithography machines: the field enhancement at the facet center, and the lens effect between the central facet area and the extractor. This is demonstrated with Fig. 16 for the growth of a facet as illustrated. The black curve in the graph gives the change in field strength at the facet center. It can be seen that the field strength goes down for increasing facet size. The associated change in practical brightness can also be calculated[14] if the operating temperature, work function, and Fermi energy are known. This result is also shown in Fig. 16 for a temperature of 1800 K, a work function of 3.04 eV, and a Fermi energy of 11.47 eV. Note that the change in the brightness is much stronger than the change in field strength. The third curve in Fig. 16 gives the associated change in angular intensity of the source, which is proportional to the probe current used in applications. It can be seen that while the facet size and brightness are changing considerably, the probe current is approximately unaffected. This is the net result of the changes in both the field strength and the lens effect: the field strength increases, but the beam divergence also increases. It can be shown that the net effect on the probe current for an increasing facet size can also be slightly increasing or slightly decreasing, depending on the exact conditions. In the experiment (Fig. 8) the biggest change in the central pattern intensity (proportional to the probe current) was in the first few hours after increasing the voltage from 2 to 6 kV. It is noted that this trend is also seen in both the screen current and the extractor current and might be ascribed to an effect different from a change in facet size. After the first few hours the changes in the central pattern intensity are small, while the screen current is clearly still increasing. The probe current is thus not necessarily a good indicator of changes in the tip geometry that induce changes in brightness and energy spread.

In summary, changing the operating voltage of a source of course changes the performance of the system instantly, but because the end facet will start changing its geometry, it can take several hours before the system is stable, and this cannot always be monitored by measuring the probe current.

VII. CONCLUSION

The properties of a probe from a Schottky emitter, such as its brightness, energy spread, and the amount of current in the probe as selected by an aperture are a function of the geometry of the emitter, and these properties are stable only when the emitter geometry is stable. It was found that the tip end geometry, and thus the probe properties, can change considerably and reproducible in response to a change in the operating conditions. The emission pattern as generated by the end facet of the emitter was found to be a useful tool to investigate this.

Changing to a lower operating voltage, the tip end will become less faceted and more rough, and the end facet will decrease in size and become more circular. Note that if the voltage is kept low enough for a long time, the end facet will start to collapse.

If the operating voltage has been low and the tip end has a low degree of faceting, an increase in the operating voltage will cause the tip end to develop more and/or larger facets, and the end facet is expected to grow in size. Once fully faceted, the geometry was found to be relatively stable if the operating conditions were kept constant. It is noted that the fully faceted geometry is not necessarily also stable in the long run because of the nonvanishing gradient in chemical potential between tip and shank. From other studies it seems that whatever happens to the details of the facet, in the long run, the tip diameter always grows over a period of years.

In theory, the geometry changes could also be exploited, e.g., to temporarily increase the brightness of the probe at a given voltage: operate the source for several hours at lower voltage to reduce the facet size and increase the field enhancement at the facet center, and then set back the voltage. The brightness of the probe will be temporarily increased and will degrade again in the next few hours. A similar strategy could serve to temporarily decrease the energy spread.

ACKNOWLEDGMENTS

The authors would like to thank Greg Schwind, Lyn Swanson, and Ted Tessner of FEI Company for the use of SEM images (in Fig. 2) and for the useful discussions.

[1] L. W. Swanson and G. A. Schwind, in *Handbook of Charged Particle Optics Second Edition*, edited by J. Orloff (CRC, New York, 2008), Chap. 1, p. 1.
[2] Yanxia Zhang and P. Kruit, J. Vac. Sci. Technol. B **25**, 2239 (2007).
[3] M. S. Bronsgeest and P. Kruit, J. Vac. Sci. Technol. B **26**, 2073 (2008).
[4] H. Ibach, Physics of Surfaces and Interfaces (Springer, Berlin, 2006), Chap. 4, p. 149.
[5] S. Fujita and H. Shimoyama, Phys. Rev. B **75**, 235431 (2007).
[6] F. A. Nichols and W. W. Mullins, J. Appl. Phys. **36**, 1826 (1965).
[7] J. P. Barbour, F. M. Charbonnier, W. W. Dolan, W. P. Dyke, E. E. Martin, and J. K. Trolan, Phys. Rev. **117**, 1452 (1960).
[8] W. P. Dyke, F. M. Charbonnier, R. W. Strayer, R. L. Floyd, J. P. Barbour, and J. K. Trolan, J. Appl. Phys. **31**, 790 (1960).

[9]P. C. Bettler and G. G. Love, J. Appl. Phys. **38**, 3835 (1967).
[10]FEI Beam Technology Division, 5350 NE Dawson Creek Dr., Hillsboro, OR 97124, USA.
[11]M. S. Bronsgeest and P. Kruit, J. Vac. Sci. Technol. B **24**, 887 (2006).
[12]Calculations performed with CPO2D of CPO programs (http://www.electronoptics.com). The facet is split up in 1 nm length charge segments. Ray tracing is done for electrons launched with zero tangential energy and 100 m/s forward energy at 2 nm from the facet. Field strength is evaluated at 2 nm from the facet.
[13]G. Fursey, in *Field Emission in Vacuum Microelectronics*, edited by I. Brodie and P. Shwoebel (Kluwer Academic, New York/Plenum, New York, 2005), Chap. 7, p. 115.
[14]B. J. Cook, M. S. Bronsgeest, C. W. Hagen, and P. Kruit, Ultramicroscopy **109**, 403 (2009).